AMERICAN SOCIETY FOR MICROBIOLOGY | Antimicrobial Agents and Chemotherapy®

MECHANISMS OF ACTION: PHYSIOLOGICAL EFFECTS

Inhibition of PfMYST Histone Acetyltransferase Activity Blocks *Plasmodium falciparum* Growth and Survival

Utsav Sen,[a] Akshaykumar Nayak,[a] Juhi Khurana,[a] Deepu Sharma,[a] Ashish Gupta[a]

[a]Epigenetics and Human Disease Laboratory, Department of Life Sciences, Shiv Nadar University, Gautam Budh Nagar, Uttar Pradesh, India

Utsav Sen and Akshaykumar Nayak are co-first authors and contributed equally to this work. Author order was determined on the basis of seniority.

ABSTRACT One of the major barriers in the prevention and control of malaria programs worldwide is the growing emergence of multidrug resistance in *Plasmodium* parasites, and this necessitates continued efforts to discover and develop effective drug molecules targeting novel proteins essential for parasite survival. In recent years, epigenetic regulators have evolved as an attractive drug target option owing to their crucial role in survival and development of *Plasmodium* at different stages of its life cycle. PfMYST, a histone acetyltransferase protein, is known to regulate key cellular processes, such as cell cycle progression, DNA damage repair, and antigenic variation, that facilitate parasite growth, adaptation, and survival inside its host. With the aim of assessing the therapeutic potential of PfMYST as a novel drug target, we examined the effect of NU9056 (an HsTIP60 inhibitor) on the rate of parasite growth and survival. In the present study, by using a yeast complementation assay, we established that PfMYST is a true homolog of TIP60 and showed that NU9056 can inhibit PfMYST catalytic activity and kill *P. falciparum* parasites in culture. Inhibiting the catalytic activity of PfMYST arrests the parasite in the trophozoite stage and inhibits its further transition to the schizont stage, eventually leading to its death. Overall, our study provides proof of concept that PfMYST catalytic activity is essential for parasite growth and survival and that PfMYST can be a potential target for antimalarial therapy.

KEYWORDS *Plasmodium*, PfMYST, NU9056, TIP60, HAT assay, *Plasmodium falciparum*, malaria

Malaria is a parasitic infectious disease that entails significant morbidity and mortality each year worldwide. Despite ongoing malaria control and eradication programs, according to the latest World Health Organization (WHO) report, nearly 405,000 people died due to malaria in 2018 from the total reported 228 million cases of malaria that occurred worldwide (1). Developing resistance in the human malaria parasite to the antimalarial drugs currently available on the market, including the most potent antimalarial drug, artemisinin, is not only obstructing the malaria control efforts but is also becoming a serious threat to human health. High treatment failure rates of artemisinin combination therapies (ACTs) in most regions where malaria is endemic (1) show the declining efficacy of ACTs and emphasize the urgent need to develop alternative antimalarial drugs or new relevant molecular targets in the parasite that can be exploited for developing new antimalarial drug candidates. It has therefore become important to refine our understanding of the parasite's complex biology in order to identify the factors that not only support its growth and survival inside the host but also contribute to pathogenesis.

The multistage life cycle of the human malaria parasite takes place within two different hosts, mosquitoes and humans. During its complex life cycle, *Plasmodium* undergoes a series of extensive biochemical and physiological transformations that

Citation Sen U, Nayak A, Khurana J, Sharma D, Gupta A. 2021. Inhibition of PfMYST histone acetyltransferase activity blocks *Plasmodium falciparum* growth and survival. Antimicrob Agents Chemother 65:e00953-20. https://doi.org/10.1128/AAC.00953-20.

Address correspondence to Ashish Gupta, ag315@snu.edu.in.

Received 11 May 2020
Returned for modification 19 June 2020
Accepted 1 October 2020
Accepted manuscript posted online 12 October 2020
Published 16 December 2020

represent functional adaptations of each developmental stage to its respective host environment. An interesting aspect of malaria parasite biology is that it can swiftly modify its epigenetic landscape to induce a rapid yet finely tuned gene expression profile, which facilitates its survival, adaptation, and development while passing through different cellular environments in different hosts (2–5). Some of the chromatin-modifying proteins regulating these epigenetic changes identified and functionally characterized in *Plasmodium* are PfGCN5 (general control nonrepressed 5), PfMYST (MOZ, Ybf2/Sas3, Sas2, and TIP60), histone lysine methyltransferase family (HKMT) proteins, etc. (6–10). Unlike for the majority of higher eukaryotes, there is still a gap of knowledge of precisely how these epigenetic factors and epigenetic factor-induced variations in chromatin modification contribute to the regulation of gene expression in *Plasmodium* and requires thorough investigation.

PfMYST, a putative homolog of human histone acetyltransferase protein TIP60 (HsTIP60), is emerging as an important factor shown to play roles in gene activation, cell cycle control, and DNA repair processes essential for parasite survival (8). PfMYST induces histone modification by acetylating histone 4 (lysine residues K5, K8, K12, and K16) (8). Recently, we also identified PfRUVBL3 as an interacting partner of PfMYST protein, and the PfMYST-PfRUVBL3 complex was shown to colocalize with H3K9me1 histone in the ring stage of the parasite, suggesting their possible role in transcriptional regulation during the *Plasmodium falciparum* intraerythrocytic developmental cycle (IDC) (11). Studies on the human genome have linked enhanced occupancy of the H3K9me1 marker with actively transcribed promoters and shown their predominant enrichment at transcription start sites (12).

Because PfMYST protein is essential for parasite survival and because it is an enzyme, we investigated its potential as a molecular target for antimalarial therapy. In the present work, we show for the first time that PfMYST is a true homolog of TIP60, as determined by using a yeast complementation assay. We show that the inhibition of PfMYST catalytic activity with NU9056 results in robust inhibition of *P. falciparum* growth followed by parasite death in *in vitro* culture. Overall, our data strongly imply that catalytic activity of PfMYST is essential for parasite survival and suggest its potential to serve as a novel molecular target for antimalarial drug design. Further, our established *in vitro* PfMYST histone acetyltransferase (HAT) assay can be exploited to identify compounds that can be developed as new antimalarials.

RESULTS

PfMYST is a true homolog of yeast Esa1 protein. Based on sequence analysis, PfMYST is considered a putative homolog of TIP60. Protein sequence analysis using Clustal Omega showed that PfMYST exhibits 39.5% and 41.4% identity with *Saccharomyces cerevisiae* (ScEsa1) and human (HsTIP60) homologs (Fig. S1A and B). Interestingly, PfMYST possesses an ~200-amino-acid long asparagine-rich stretch in its N-terminal region. Domain analysis of PfMYST showed that it is composed of a characteristic chromodomain and a catalytic MYST domain (Fig. S1C). We therefore wanted to determine whether PfMYST is a true homolog of TIP60. In yeast, Esa1 is a homolog of TIP60 protein and is shown to be essential for survival (13). To analyze whether PfMYST protein complemented the functions of Esa1 protein, we generated clones of ScEsa1 and PfMYST in the yeast expression vector pRS314 (Fig. S2) and performed complementation assays in a yeast Esa1 temperature-sensitive strain. *S. cerevisiae* LPY3500 grows normally at a permissible temperature (25°C) but fails to grow at a restrictive temperature (37°C) due to degradation of endogenous Esa1 protein (13). The Esa1 temperature-sensitive strain was transformed with the vector pRS314-PfMYST, pRS314-ScEsa1, or pRS314 vector, and transformed cells were incubated at 25°C and 37°C. All the transformed yeast strains grew normally at 25°C; however, at 37°C, only the transformed yeast strain carrying the ScEsa1 or PfMYST plasmid could survive and grow (Fig. 1A). Under similar conditions, a yeast strain transformed with pRS314 vector alone failed to survive at 37°C (Fig. 1A). Western blot analysis of transformed yeast strains showed expression of recombinant PfMYST protein from pRS314-PfMYST plasmid

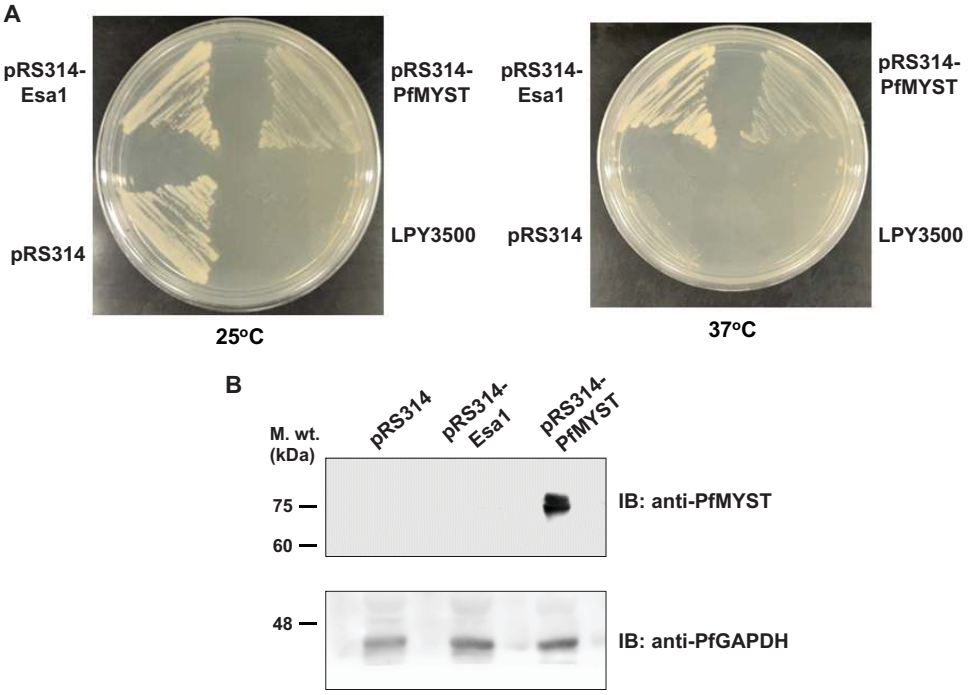

FIG 1 PfMYST is a true homolog of the yeast protein Esa1. (A) For the complementation assay, a yeast temperature-sensitive strain (LPY 3500) was transformed with plasmids pRS314, pRS314-ScEsa1, and pRS314-PfMYST using the lithium chloride method. Transformed cells were incubated on tryptophan dropout medium plates for 3 to 4 days at 25°C. Replica plates were streaked with colonies and incubated at 25°C and 37°C for 3 to 4 days. (B) A Western blotting assay was performed to detect the expression of PfMYST in transformed yeast cells. Lysates of pRS314-, pRS314-ScEsa1-, and pRS314-PfMYST-transformed yeast cells were resolved by SDS-PAGE, and Western blot analysis was performed using anti-PfMYST antibody or anti-PfGAPDH antibody.

(Fig. 1B). Together, these results show that PfMYST protein can complement the functions of yeast protein Esa1 and thus is a true homolog of TIP60.

Recombinant PfMYST protein is catalytically active. Since MYST family proteins have HAT domains that can catalyze the transfer of the acetyl coenzyme A moiety to lysine residues of substrate proteins, we wanted to determine the HAT activity of full-length PfMYST protein. Our lab previously reported the purification of full-length recombinant PfMYST protein under native conditions from bacteria (11), and in the present study, we wanted to determine whether this bacterially purified recombinant glutathione *S*-transferase (GST)-PfMYST protein possessed HAT activity. For this, GST-PfMYST or GST protein was purified from bacteria under native conditions by affinity chromatography using GST beads (Fig. S3). An *in vitro* HAT assay was performed using mammalian H4 histone as the substrate. Western blot analysis performed with anti-acetyl lysine H4 antibody showed signal in samples containing GST-PfMYST recombinant protein only (Fig. 2A). Under similar conditions, samples incubated with GST protein failed to show any signal with acetylated lysine antibody. Western blotting with anti-H4 antibody used as a control showed a single band at the expected size of histone H4, indicating equal loading of the reaction samples (Fig. 2A).

To validate the role of the HAT domain in the observed *in vitro* HAT activity of GST-PfMYST protein, we generated a catalytically dead version of PfMYST protein by mutating Q377 and G380 to E (glutamine to glutamic acid and glycine to glutamic acid) located in its HAT domain through site-directed mutagenesis (14). Clustal W analysis of HsTIP60 and PfMYST proteins showed that both Q377 and G380 are conserved in the PfMYST catalytic domain (Fig. S1). A schematic representation of mutations is presented in Fig. 2B. Point mutations were generated in the full-length PfMYST open reading frame (ORF), and the resulting double mutant was cloned into pGEX-6p2 vector. Recombinant GST-PfMYST (HAT mutant) protein was purified from bacteria under

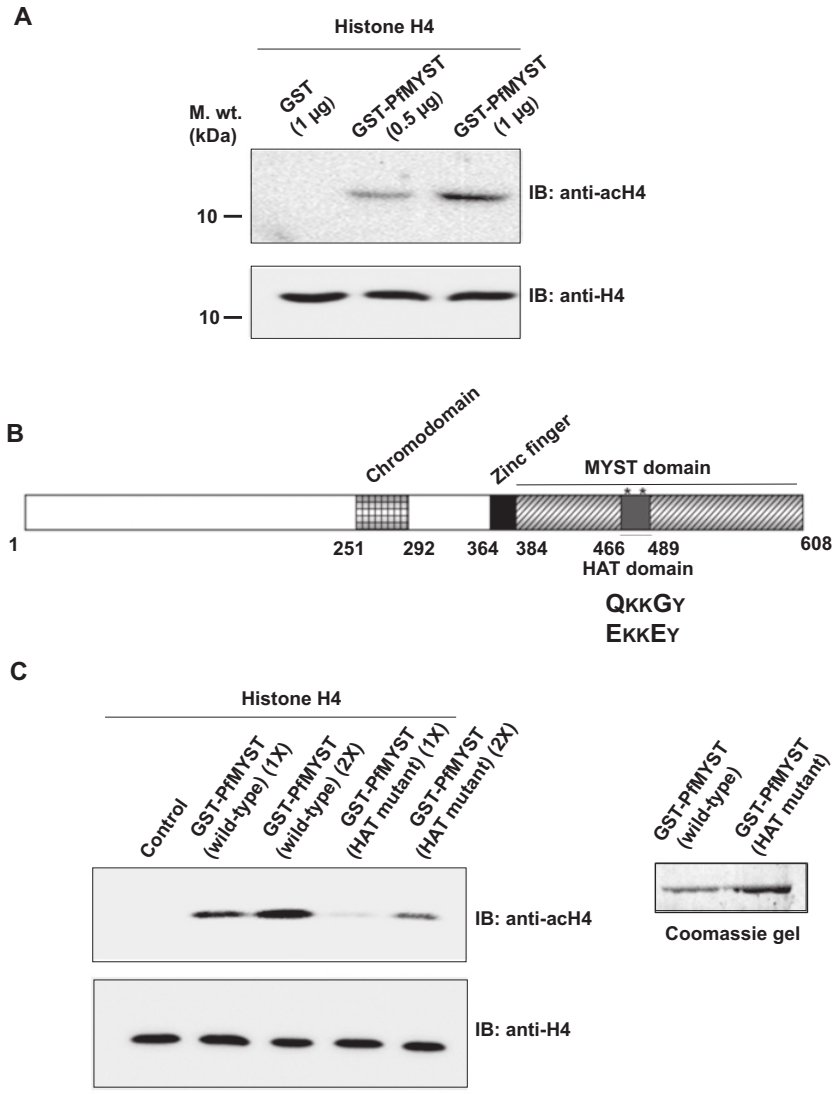

FIG 2 Recombinant PfMYST displays HAT activity *in vitro*. (A) Purified GST and GST-PfMYST proteins were used for an *in vitro* HAT assay using recombinant human histone 4 (H4) protein as the substrate. The reaction was stopped by boiling samples at 95°C with 2× Laemmli sample buffer and resolved by SDS-PAGE followed by Western blotting using anti-acetylated histone 4 and anti-histone 4 antibodies. (B) Schematic diagram depicting mutations generated in the HAT domain of PfMYST. (C) A HAT assay was performed with 500 ng (1X) and 1 μg (2X) of purified GST-PfMYST (wild type) and GST-PfMYST (HAT mutant) protein, as mentioned earlier. Western blot analysis was performed with anti-acetylated histone 4 and anti-histone 4 antibodies. Coomassie staining of the gel showed purified GST-PfMYST (wild type) and GST-PfMYST (HAT mutant) proteins.

native conditions by affinity chromatography using GST beads, similar to GST-PfMYST (wild-type) protein (data not shown). An *in vitro* HAT assay was performed using GST-PfMYST (wild-type) protein or GST-PfMYST (HAT mutant) protein. Western blot analysis of reaction samples with anti-acetyl lysine H4 antibody showed increasing signal with increasing concentration of GST-PfMYST (wild-type) protein (Fig. 2C). On the other hand, there was a significant decrease in the H4 acetylation levels in the reaction samples incubated with similar concentrations of GST-PfMYST (HAT mutant) protein under similar conditions (Fig. 2C). Western blotting with anti-H4 histone antibody showed equal loading of the reaction mixture in all the lanes. Overall, these results show that recombinant PfMYST full-length protein purified from bacteria displays HAT activity that is dependent on its catalytic domain.

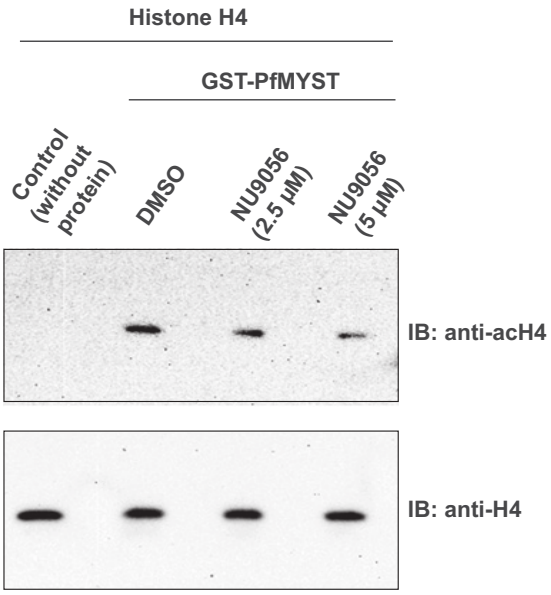

FIG 3 NU9056 inhibits PfMYST HAT activity. *In vitro* HAT assay was performed with GST-PfMYST recombinant protein in the presence of DMSO or NU9056. Reaction samples were resolved by SDS-PAGE and Western blotting was performed using anti-acetylated histone 4 antibody to determine H4 acetylation levels. The Western blot with anti-histone 4 antibody shows equal loading of samples. The faint vertical line visible in the blot is due to an equipment glitch.

NU9056 inhibits catalytic activity of PfMYST *in vitro*. After establishing an *in vitro* assay for measuring HAT activity of recombinant PfMYST protein, we were interested in examining the effect of NU9056 [5-(1,2-thiazol-5-yldisulfanyl)-1,2-thiazole, a well-known inhibitor of HsTIP60 catalytic HAT activity] on PfMYST catalytic activity (15). To examine the effect of NU9056 on catalytic activity of PfMYST, we performed an *in vitro* HAT assay with recombinant GST-PfMYST protein with dimethyl sulfoxide (DMSO) (control) or NU9056. Western blot analysis performed with anti-acetyl lysine H4 antibody showed significant decrease in HAT activity of PfMYST with increasing concentrations of NU9056 (Fig. 3). Western blot analysis with anti-H4 antibody showed similar intensity signals in all lanes, indicating equal loading of the reaction samples. This result shows that NU9056 can significantly inhibit the catalytic HAT activity of PfMYST.

NU9056 inhibits IDC progression and causes parasite death. Since NU9056 could inhibit the catalytic activity of PfMYST protein, we next wanted to examine the impact of NU9056-induced inhibition of PfMYST catalytic activity on the growth and survival of *Plasmodium*. For this, a synchronized *Plasmodium* culture in the ring stage was incubated with DMSO or NU9056, and parasitemia was measured at regular time intervals. A graph was plotted for the obtained values, which showed a drastic decrease in parasitemia in NU9056-treated samples compared to controls (Fig. 4A). To analyze the effect of NU9056 on IDC progression, surviving parasites in different stages of the IDC were counted. Result showed that more than 80% of parasites treated with NU9056 were arrested in the trophozoite stage and could not complete the IDC even after 48 h of treatment; however, under similar conditions, DMSO-treated parasites completed the IDC and started a new round of the infection cycle (Fig. 4B). Upon Giemsa staining, NU9056-treated parasites showed abnormal morphology indicative of parasites under stress (Fig. 4C). Since NU9056 showed a drastic effect on parasite growth and survival, we wanted to determine whether NU9056 has any effect on the expression level of PfMYST protein. Western blot analysis was performed with 0-h and 48-h DMSO- and NU9056-treated samples using anti-PfMYST antibody. The results showed that PfMYST protein levels were similar in DMSO- and NU9056-treated samples (Fig. 4D). This suggests that NU9056-dependent parasite inhibition was due to blockage of PfMYST catalytic activity and not due to depletion of PfMYST. Titration analysis of NU9056 was

A

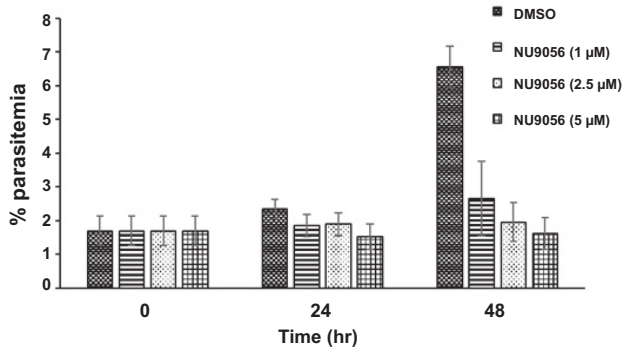

B

Time (post drug treatment)	0 hour			48 hour		
Parasite stages (%)	Ring	Trophozoite	Schizont	Ring	Trophozoite	Schizont
DMSO	94.2 (±1.01)	5.51 (±1.01)	0	75.61 (±1.01)	19.59 (±1.19)	5.12 (±1.01)
NU9056 (1 μM)	91.38 (±1.41)	9.01 (±1.24)	0	15.16 (±0.61)	80.71 (±1.22)	4.39 (±0.41)
NU9056 (2.5 μM)	93.46 (±0.87)	6.77 (±1.19)	0	6.63 (±0.34)	87.50 (±0.74)	6.41 (±0.66)
NU9056 (5 μM)	92.84 (±0.12)	7.39 (±0.13)	0	5 (±0.81)	91.54 (±1.91)	4.1 (±1.78)

C

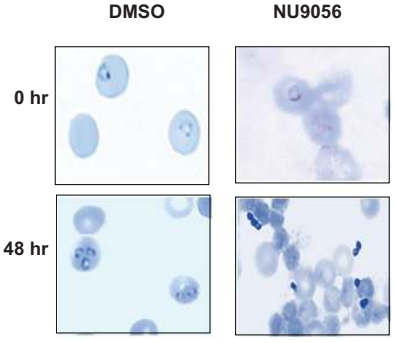

D

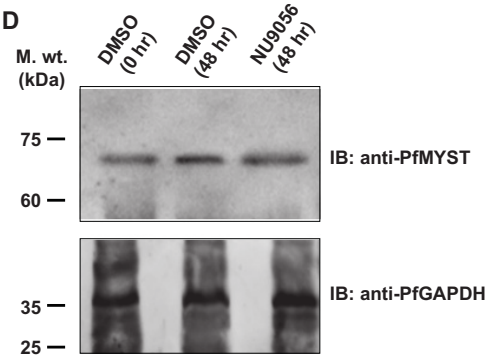

FIG 4 NU9056 inhibits *Plasmodium* growth and survival. (A) Synchronized parasite cultures were treated with either DMSO or NU9056, and Giemsa-stained slides were prepared at 0, 24, and 48 h posttreatment. Parasitemia was calculated for each time point, and the graph was plotted with the average values from three independent experiments performed in duplicate, with standard deviations (SD). (B) Effect of NU9056 on parasite growth. Synchronized ring-stage cultures were treated with the indicated amounts of DMSO or NU9056, and the percentage of surviving parasites at different stages of the IDC were calculated. Value are averages from three independent experiments, with SD. (C) Giemsa-stained images show the morphology of parasites in control (DMSO-treated) and NU9056-treated parasites at 0 and 48 h posttreatment. (D) Western blot analysis was performed to determine the effect of NU9056 on PfMYST expression levels in the parasite. Lysates of DMSO- and NU9056-treated parasites from the indicated posttreatment time points were resolved by SDS-PAGE followed by Western blotting with anti-PfMYST antibody. Western blot analysis with anti-PfGAPDH antibody shows the loading control.

performed in *Plasmodium* cultures, and the 50% inhibitory concentration (IC_{50}) of NU9056 was calculated to be 0.9 μM using GraphPad Prism 5.0 (Fig. S4). We did not observe any significant toxicity at this concentration of NU9056 for human erythrocytes in an *in vitro* culture (data not shown). Together, all these results show that NU9056 can block the parasite's IDC progression in the trophozoite stage, which eventually causes stress in the parasite, resulting in its death.

PfMYST displays substantial structural differences from its human homolog. Our results showed that inhibiting PfMYST activity leads to parasite death. Since PfMYST is a homolog of HsTIP60 and both proteins exhibit similar enzymatic activities, to exploit PfMYST as an antimalarial target, it is important to establish structural-level differences between the proteins. Domain comparison of PfMYST with HsTIP60 showed that PfMYST contains a characteristic chromodomain and a MYST domain but lacks the NR box domain and has a distinct long N-terminal extension (Fig. 5A). Full-length structures of both PfMYST and HsTIP60 proteins were generated using the Rosetta-based Robetta web server by the comparative modeling method. To validate the structures, the models generated were further analyzed for stereochemical and overall quality using ProSA, VERIFY3D, ERRAT, and PROCHECK. The stereochemical quality of the full-length structures with the PROCHECK Ramachandran plot was found to be good, with 92.8% residues in most favored regions, 7.2% in additional allowed regions, and 0.0% in disallowed regions for HsTIP60. In the case of PfMYST, 90.2% of residues fall in most favored regions, 8% in additional allowed regions, and 0.9% in disallowed regions. The overall quality (ERRAT score) of 94.8 and 88.135 for HsTIP60 and PfMYST, respectively, is high enough for a reasonable model. VERIFY3D values of 85.19% for HsTIP60 and 87.5% for PfMYST also confirmed the high quality of structures. The Z scores of ProSA for HsTIP60 and PfMYST were −9.12 and −9.11, respectively, which is within the range observed for a native set of proteins of the same size.

Similarly, 3D structures of the MYST domain for PfMYST and HsTIP60 were generated by MODELLER 9.21. The stereochemical quality of the structures with PROCHECK Ramachandran plot was found to be good, with 91.3% residues falling in most favored regions, 8.2% in additional allowed regions, and 0.5% in disallowed regions for the MYST domain of PfMYST and with 93.6% of residues in most favored regions, 6.4% in additional allowed regions, and 0.0% in disallowed regions for the MYST domain of HsTIP60. These structures were also validated using ProSA, VERIFY3D, and ERRAT. The Z scores of ProSA for PfMYST and HsTIP60 were −6.61 and −6.98, respectively, which is within the range observed for a native set of proteins of the same size. A VERIFY3D value of 96.39% for both PfMYST and HsTIP60 also confirmed the high quality of the structures. The overall quality (ERRAT score) of 95 for both PfMYST and HsTIP60 is high enough for a reasonable model. MYST domain structures of PfMYST and HsTIP60 proteins were also generated by SWISS-MODEL. The stereochemical quality of the structures generated with SWISS-MODEL server, as checked using PROCHECK Ramachandran plot, was found to be good, with 92.2% of residues in most favored regions, 7.8% in additional allowed regions, and 0.0% in disallowed regions for the MYST domain of HsTIP60. Similarly, for the MYST domain of PfMYST, 96% of residues fall in most favored regions, 4% in additional allowed regions, and 0.0% in disallowed regions. The overall quality (ERRAT score) of 98.87 and 96.98 for catalytic domain of HsTIP60 and PfMYST, respectively, is high enough for a reasonable model. A VERIFY3D value of 93.16% for HsTIP60 and 87.16% for PfMYST also confirmed the high quality of structures for the MYST domain. The Z scores of ProSA for HsTIP60 and PfMYST were −6.44 and −6.78, respectively, which is within the range observed for a native set of proteins of the same size.

The superimposed structure for full-length PfMYST and HsTIP60 showed a root mean square deviation (RMSD) of 21.544 Å and template modeling (TM) value of 0.466, indicating a high degree of structural dissimilarity between PfMYST and HsTIP60 (Fig. 5B). The N-terminal region of PfMYST (amino acids 1 to 201) displayed a unique tertiary structure, accounting for the major dissimilarity observed between three-dimensional (3D) structures of both proteins (Fig. 5B). Interestingly, in contrast to full-length structures, structural analysis of the MYST domain for both proteins showed an RMSD value of 5.201 Å and a TM value of 0.715, indicating structural similarity (Fig. 5C). We got similar results with SWISS-MODEL server, which showed similarities in the catalytic domain structure of both the proteins (Fig. S5). Together, these results show that although the catalytic domain of PfMYST is similar to that of HsTIP60, its N-terminal region has a peculiar structure unrelated to that of its human homolog.

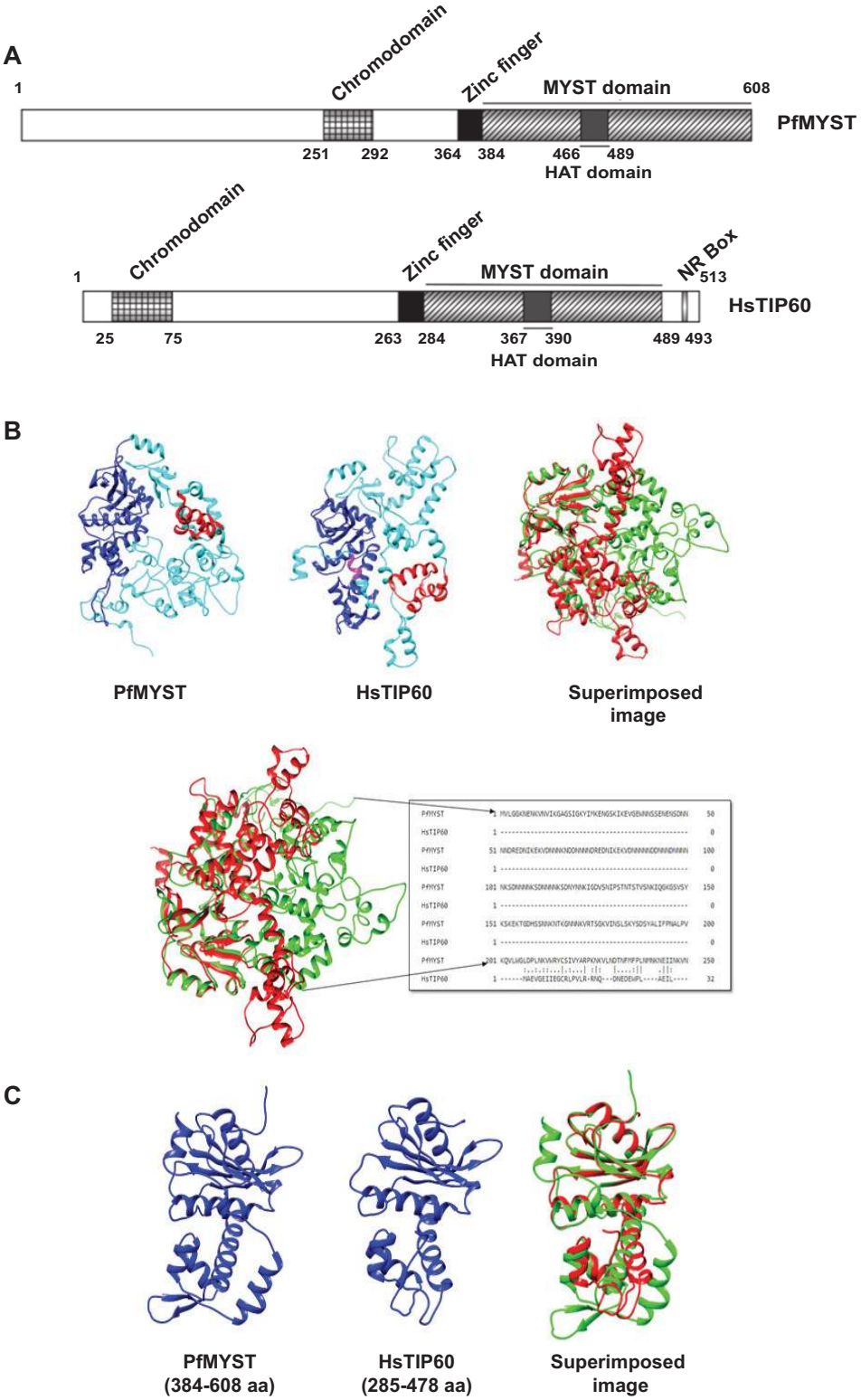

FIG 5 Ribbon diagrams of the 3D modeled structure of PfMYST and HsTIP60. (A) Schematic diagrams depicting the domain organization of PfMYST and HsTIP60. (B) Structures generated by comparative modeling of full-length PfMYST and HsTIP60 proteins. The chromodomain region is in red, the MYST domain is in blue and the NR box of HsTIP60 is in magenta. The superimposition of PfMYST (green) and HsTIP60 (red) structures was performed by using the MatchMaker function of UCSF Chimera. (C) Ribbon representation of the 3D-modeled structure for the catalytic MYST domain of PfMYST and HsTIP60. Catalytic MYST domain structures of PfMYST (384 to 608 amino acids) and HsTIP60 (285 to 478 amino acids) were generated using MODELLER 9.21 based on the homology modeling method. Superimposition of the MYST domains of PfMYST (green) and HsTIP60 (red).

DISCUSSION

Genome-wide studies have made significant contributions to our understanding of the epigenetic mechanisms regulating the dynamics of gene expression and morphological transformations in *Plasmodium* and their functional impact on virulence and malaria pathogenesis (16–18). The complicated life cycle of the malaria parasite demands appropriate and precise expression of genes at the right moment to support its growth and survival. Studies provide convincing evidences that chromatin modifiers and epigenetic events play a key role in modulating gene expression critical to different aspects of malaria parasite physiology and pathogenesis (18–20). Although this field is in its infancy, a repertoire of ATP-dependent chromatin remodelers and histone-modifying enzymes identified in *Plasmodium* have emerged as a promising drug targets and are now being exploited for screening and identification of novel antimalarial compounds (9, 21, 22). PfMYST is one such essential HAT protein that is known to regulate important processes of the parasite, including cell cycle control, gene transcription, antigenic variation, and DNA repair (8).

Because of the reported significance of PfMYST in regulating important processes of the parasite, we wanted to investigate its potential as a possible drug target for antimalarial drug screening and identification. Using *in silico* analysis and yeast complementation assays, we found that PfMYST shows a closer resemblance in the identity matrix to human TIP60 than to yeast Esa1 and is a true homolog of the eukaryotic TIP60 protein. This is in contrast to a previous study by Miao et al., which failed to show functional complementation of *S. cerevisiae* by PfMYST (8). This could be because they used an N-terminal deletion version of PfMYST instead of full-length PfMYST protein for complementation studies. Interestingly, the truncated versions of PfMYST retained catalytic HAT activity but failed to rescue the transformed yeast cells in complementation assays. A study on ScEsa1 protein showed an essential role of the N-terminal region for execution of its functions (23). Thus, the N-terminal region of PfMYST may have hitherto-unexplored essential functions other than the catalytic HAT activity effected by the HAT domain located in the C-terminal region. One curious feature of the N terminus of PfMYST is the presence of a long unique stretch rich in asparagine repeats. Many proteins in *Plasmodium* are known to have low-complexity repetitive regions; proteins with asparagine repeats have a propensity to form aggregates and parasite chaperons can stabilize these proteins (24). In addition, the presence of only one $tRNA^{Asn}$ gene and low levels of asparaginylated $tRNA^{Asn}$ is suggested to slow the translation rate of asparagine-rich proteins (25). This indicates that the malaria parasite could regulate the expression of proteins rich in asparagines by multiple mechanisms. We have published a study showing interaction of PfRUVBL3 (AAA family member protein) with PfMYST (11). RUVBL proteins are also known to act as chaperones. In humans, RUVBL1 and -2 are required for active TIP60 complex formation and activity (26). Similarly, PfRUVBL1, -2, and -3 might act as chaperones for PfMYST. Since overexpression of PfMYST has been shown to disrupt the cell cycle (8), we speculate that presence of an asparagine-rich region in PfMYST might be responsible for controlling its expression and interaction with other proteins that might further fine-tune its cellular functions.

To ensure that the recombinant PfMYST protein was catalytically active, we performed an *in vitro* HAT assay and observed that recombinant PfMYST protein could successfully acetylate its substrate, histone H4. Although the comparative sequence analysis of full-length PfMYST revealed 41% identity with human TIP60, the catalytic MYST domain sequences of PfMYST revealed high conservation with human TIP60. A more detailed comparison of the MYST domain sequence of five main *Plasmodium* spp. (that are known to infect humans and cause disease) revealed a high sequence similarity in the MYST domain, indicating evolutionarily conserved functional significance of this protein in *Plasmodium* (Fig. S6). Our study demonstrated that mutation of two conserved residues located in the catalytic domain of PfMYST renders it catalytically dead. Amino acid sites for mutational studies were selected based on the

conserved and critical nature of these residues in human TIP60 for its catalytic activity and intranuclear organization. Thus, these results not only showed the robustness of our assay but also indicated an analogous mode of enzymatic action of both proteins.

Considering the essential role of PfMYST in processes vital for the survival of parasite, we postulated that inhibiting its catalytic activity must prove lethal for the parasite. To evaluate this possibility, we tested the effect of NU9056 on PfMYST catalytic activity and parasite growth rate. NU9056 (an isothiazolone compound) has been shown to be a specific inhibitor of human TIP60. Inhibition of HsTIP60 catalytic HAT activity by NU9056 results in alteration in the localization pattern of HsTIP60 protein and inhibition of cell proliferation (14, 15). Our *in vitro* HAT assay data clearly showed that NU9056 significantly inhibits PfMYST catalytic activity. Also, addition of NU9056 to the synchronized parasite culture showed stage-specific arrest of parasite growth in the trophozoite stage, which eventually leads to parasite death. Interestingly, the concentration of NU9056 required to inhibit *Plasmodium* growth by 50% in *in vitro* culture was found to be 0.9 μM, which is quite low compared to the concentration of NU9056 shown to result in 50% inhibition in different prostate cancer cell lines, with a concentration range of 8 to 27 μM (15). According to a report by Miao and coworkers, the total acetylation of *Plasmodium* proteins drastically increases during the trophozoite stage, and proteins related to histone, transcription, and metabolism are abundantly acetylated during this period (27). It is also noteworthy that TIP60 is a critical hub protein that plays a role in many important cellular processes by acetylating histone and many nonhistone proteins (28, 29). Since PfMYST is a homolog of TIP60 in the parasite, it could also have a role as a hub protein, and PfMYST catalytic activity might be essential for PfMYST-dependent acetylation of proteins whose functions are important for parasite growth and development in the trophozoite stage as well as in progression of the parasite from the trophozoite to the schizont stage. Our study clearly demonstrates that small molecule inhibitors like NU9056 can target PfMYST and that this inhibition is lethal for the parasite. Our *in silico* structural analysis also revealed uniqueness in the PfMYST structure that can be exploited for computational screening of new biological safe compounds specific against PfMYST.

HAT-mediated acetylation of histone serves as a crucial means of introducing flexible alterations in chromatin to modulate the pattern of gene expression. Hence, it is not surprising that deregulated or compromised catalytic activity of these enzymes can have profound effects on the expression of genes involved in diverse biological processes and can lead to a variety of disease conditions. In recent years, epigenetic regulators such as DNA methyltransferases (DNMTs), histone deacetylases (HDACs), and HATs have emerged as important classes of drug target candidates (30, 31). Indeed, FDA-approved drugs like 5-Aza-CR593 and 5-Aza-CdR594, used for the treatment of chronic myelomonocytic leukemia, and valproic acid for the treatment of epilepsy are epigenetic modulators. In addition, several small molecular compounds targeting HATs and HDACs are undergoing clinical trials (32). However, due to the broad range of side effects associated with the use of epigenetic drugs, rigorous *in vitro* and *in vivo* testing and careful assessment of the risk-benefit relationship are needed to improve the likelihood that a preclinical drug will receive approval for clinical consideration (33).

However, in order to exploit the pharmacological benefit of PfMYST as a novel target for antiplasmodial therapy, high-throughput screening and robust *in vitro* assays are needed to identify highly potent and selective modulator of PfMYST, followed by stringent testing in *in vivo* models. Since PfMYST is identified as an essential epigenetic factor for *Plasmodium* survival, specific inhibitors of PfMYST could also help in understanding the basic biology of *Plasmodium* with respect to the epigenetics mechanisms controlling its growth and survival.

Overall, the findings of this study provide a proof of concept that modulation of an epigenetic regulator, in this case, PfMYST, could be of potential therapeutic benefit in controlling parasite growth; however, there is still a long way to go before this protein could in reality be targeted for antimalarial therapy.

MATERIALS AND METHODS

DNA manipulations. pGEX6p2-PfMYST (wild-type) clone was generated in the lab previously (11). pGEX6p2-PfMYST (HAT mutant) clone was generated by introducing point mutations (Q377E and G380E) in the PfMYST (wild-type) open reading frame (ORF) by overlap extension PCR (OE-PCR) using specific primers (primers P1 and P2 and primers P3 and P4) (Table S1). The amplified mutated ORF was cloned into the pGEX-6P2 vector to generate the pGEX-6P2-PfMYST (HAT mutant) construct.

To generate the pRS314-ScEsa1 clone, full-length ScEsa1 ORF was amplified using pRSETc-ESA1 plasmid (a kind gift from Lorraine Pillus, University of California at San Diego, La Jolla, CA) and specific primers P5 and P6 (Table S1). The amplified ORF was cloned into the pRS314 vector in the galactose-inducible cassette under the BamHI and EcoRI restriction enzyme sites to generate the pRS314-ScEsa1 clone. To generate the pRS314-PfMYST clone, PfMYST ORF was subcloned from the pGEX6p2-PfMYST clone into the pRS314 vector under the BamHI and EcoRI restriction enzyme sites.

Yeast complementation assay. The *S. cerevisiae* Esa1 temperature-sensitive strain (LPY3500) (a kind gift from Lorraine Pillus, University of California at San Diego, La Jolla, CA) was transformed with pRS314, pRS314-ScEsa1, or pRS314-PfMYST constructs using the lithium chloride method. Transformed yeast cells were plated on tryptophan dropout medium plates and incubated at 25°C for 4 to 5 days. Transformed colonies were streaked on tryptophan dropout medium plates and incubated at the permissive temperature (25°C) or the restrictive temperature (37°C) for 3 to 4 days.

Parasite culture. *P. falciparum* strain 3D7 was cultured and maintained in human erythrocytes in RPMI 1640 medium supplemented with 0.5% Albumax, 0.2% $NaHCO_3$, 10 μg/ml gentamicin sulfate, and 50 μg/ml hypoxanthine in a mixed-gas environment of 90% N_2, 5% CO_2, and 5% O_2. To visualize the morphology and parasitemia of the parasites, smears of the infected erythrocytes were prepared on glass slides and stained with Giemsa dye.For synchronization of the parasite culture, ring stage parasites from 5 to 6% parasitemia were treated with 5% (wt/vol) sorbitol (137 mM NaCl, 10 mM sodium phosphate, 2.7 mM KCl [pH 7.4]) at 37°C for 10 min, followed by one wash with 1× phosphate-buffered saline (PBS) and two washes with complete RPMI medium. Parasites were subsequently incubated in complete RPMI medium to recover from the sorbitol-associated stress.

Expression and purification of GST-tagged recombinant proteins from bacteria. To express and purify GST-tagged recombinant proteins from bacteria, *Escherichia coli* BL21 cells were transformed with pGEX6p2, pGEX6p2-PfMSYT (wild type), or pGEX6p2-PfMSYT (HAT mutant) clones and were grown in LB medium containing ampicillin (100 μg/ml) until the optical density at 600 nm (OD_{600}) reached 0.6. The expression of the recombinant protein was induced with 1 mM isopropyl β-D-1-thiogalactopyranoside (IPTG) for 12 h at 37°C with constant shaking. Induced bacterial cells were harvested and lysed in lysis buffer (1× PBS, 2 mM EDTA, 5 mM dithiothreitol [DTT], 1% Triton X-100, 10% glycerol, 0.5 mM phenylmethylsulfonyl fluoride [PMSF]). Equilibrated glutathione *S*-transferase (GST) agarose beads were added to the supernatant and incubated at 4°C for 1 h with continuous rotation, followed by three washes with wash buffer (1× PBS, 5 mM DTT, 300 mM NaCl). Proteins were eluted from the beads in elution buffer (0.05 M Tris-Cl [pH 8.0], 10% glycerol, 150 mM NaCl, 20% NP-40, 20 mM glutathione, 10 mM DTT) at 4°C for 30 min. Eluted recombinant proteins were collected and dialyzed with dialysis buffer (50 mM Tris-Cl [pH 8.0], 10% glycerol, 0.1 mM EDTA, 1 mM DTT, 0.2 mM PMSF) and stored in aliquots at −80°C. GST-PfMYST (wild type), GST-PfMYST (HAT mutant), and GST recombinant proteins were purified using this method.

Western blot assay. Western blot analysis was performed to examine the expression of recombinant or endogenous proteins. Proteins were resolved in an SDS-polyacrylamide gel and than transferred to a PVDF (polyvinylidene difluoride) membrane using a Bio-Rad Trans-Blot SD semidry transfer apparatus. Following transfer, the membrane was blocked with 5% skim milk for 1 h at room temperature, followed by washing with 1× PBS-T (PBS containing Tween 20, a nonionic mild detergent) three times. Membranes were incubated first with preimmune sera or primary antibodies against PfMYST (1:500; generated in-house), PfGAPDH (1:1,000; generated in-house), and GST (1:1,000; Santa Cruz Biotechnology, Inc., USA) at 4°C for 10 to 12 h and then with corresponding secondary antibodies (anti-rabbit immunoglobulin [1:5,000] or anti-mouse immunoglobulin [1:5,000]; Santa Cruz Biotechnology, Inc., USA) for 1 h at room temperature. The membrane was then washed three times with 1× PBS-T, and signal was developed using an enhanced chemiluminescence (ECL) reagent (Bio-Rad) with a FluorChem E system (ProteinSimple).

HAT assay. The HAT assay was performed as described elsewhere (14). Recombinant proteins (GST, GST-PfMYST [wild type], and GST-PfMYST [HAT mutant]) were dialyzed in HAT buffer containing 50 mM Tris-Cl [pH 8.0], 10% glycerol, 0.1 mM EDTA, 1 mM DTT, and 0.2 mM PMSF. The HAT reaction mixture was made in a 50-μl volume by adding purified enzyme, recombinant mammalian H4 histone peptide (0.5 μg) (Millipore), acetyl coenzyme A (100 μM), and HAT buffer (50 mM Tris-Cl [pH 8.0], 10% glycerol, 0.1 mM EDTA, 1 mM DTT), and the reaction was carried out at 30°C for 1 h and subsequently stopped by adding 2× Laemmli buffer. The reaction samples were resolved by 15% SDS-PAGE followed by Western blotting with anti-acetylated histone H4 antibody (1:1,000) (Millipore) or anti-histone H4 antibody (1:2,000) (Millipore).

***P. falciparum* growth inhibition assay.** A synchronized ring stage parasite culture with ~1% parasitemia was seeded onto 6-well plates and treated with DMSO (control) or NU9056 (Tocris Bioscience, UK) in complete RPMI medium, and treated cultures were maintained for the next 48 h. Infected blood samples were harvested at regular time intervals to monitor parasitemia and morphology by Giemsa staining.

Sequence alignment, structure modeling, and structure superimposition. Multiple-sequence alignment and an identity matrix were generated using Clustal Omega software to investigate the sequence identity among PfMYST, ScEsa1, and HsTIP60 proteins. To infer the structural organization of

PfMYST and HsTIP60, 3D structure prediction for full-length HsTIP60 and PfMYST was performed by the comparative modeling approach using the Rosetta-based Robetta web server (34). The template used for modeling of HsTIP60 structure was "Acetyltransferase domain of Human HIV-1 Tat interacting protein, 60 kDa, isoform 3" (PDB ID 2OU2), with 99.64% identity and 54% coverage. PfMYST structure was modeled using "HBO1 is required for the maintenance of leukemia stem cells" as the template (PDB ID 6MAJ), with 53.68% identity and 37% coverage. Modeled structures were further refined using the Galaxy Refine server.

Structures of the MYST domains of HsTIP60 and PfMYST were modeled using MODELLER 9.21 and the SWISS-MODEL server based on the homology modeling method (35, 36). "Crystal structure of yeast Esa1 E338Q HAT domain bound to coenzyme A with active site lysine acetylated" (PDB ID 3TO9) was used as a template, with 47.93% identity and 95% coverage for MYST domain of PfMYST. Human TIP60 MYST domain was modeled using "Acetyltransferase domain of Human HIV-1 Tat interacting protein, 60 kDa, isoform 3" (PDB ID 2OU2) as the template, with 99.48% identity and 100% coverage. Modeled structures were further refined using the Galaxy Refine server.

Structure visualization and preparation and superimposition of modeled structures HsTIP60 and PfMYST were performed using UCSF Chimera (37).

SUPPLEMENTAL MATERIAL

Supplemental material is available online only.

SUPPLEMENTAL FILE 1, PDF file, 0.7 MB.

ACKNOWLEDGMENTS

We thank Lorraine Pillus (University of California at San Diego, La Jolla, California, USA) for providing the Esa1 temperature-sensitive yeast strain and the pRSETc-ESA1 clone. U.S. and D.S. thank SNU, while A.N. and J.K. thank CSIR and ICMR, respectively, for fellowships. A.G. is an Innovative Young Biotechnologist Awardee (IYBA, DBT). This study was financially supported by funding from Department of Biotechnology DBT-IYBA grant (BT/08/IYBA/2014-4). The funder had no role in study design, data collection and interpretation or the decision to submit the work for publication.

Study concept and design: A.G.; acquisition of data: U.S., A.N., J.K., D.S.; analysis and interpretation of data: U.S., A.N., J.K., D.S., A.G.; drafting of manuscript: U.S., J.K., A.G.

We declare no competing or financial interests.

REFERENCES

1. World Health Organization. 2019. World malaria report. https://www.who.int/malaria/publications/world-malaria-report-2019/en/.
2. Cui L, Jun Miao J. 2010. Chromatin-mediated epigenetic regulation in the malaria parasite Plasmodium falciparum. Eukaryot Cell 9:1138–1149. https://doi.org/10.1128/EC.00036-10.
3. Gupta AP, Bozdech Z. 2017. Epigenetic landscapes underlining global patterns of gene expression in the human malaria parasite, Plasmodium falciparum. Int J Parasitol 47:399–407. https://doi.org/10.1016/j.ijpara.2016.10.008.
4. Batugedara G, Lu XM, Bunnik EM, Le Roch KG. 2017. The role of chromatin structure in gene regulation of the human malaria parasite. Trends Parasitol 33:364–377. https://doi.org/10.1016/j.pt.2016.12.004.
5. Arama C, Quin JE, Kouriba B, Östlund Farrants AK, Troye-Blomberg M, Doumbo OK. 2018. Epigenetics and malaria susceptibility/protection: a missing piece of the puzzle. Front Immunol 9:1733. https://doi.org/10.3389/fimmu.2018.01733.
6. Fan Q, An L, Cui L. 2004. Plasmodium falciparum histone acetyltransferase, a yeast GCN5 homologue involved in chromatin remodeling. Eukaryot Cell 3:264–276. https://doi.org/10.1128/ec.3.2.264-276.2004.
7. Cui L, Fan Q, Cui L, Miao J. 2008. Histone lysine methyltransferases and demethylases in Plasmodium falciparum. Int J Parasitol 38:1083–1097. https://doi.org/10.1016/j.ijpara.2008.01.002.
8. Miao J, Fan Q, Cui L, Li X, Wang H, Ning G, Reese JC, Cui L. 2010. The MYST family histone acetyltransferase regulates gene expression and cell cycle in malaria parasite Plasmodium falciparum. Mol Microbiol 78:883–902. https://doi.org/10.1111/j.1365-2958.2010.07371.x.
9. Kanyal A, Rawat M, Gurung P, Choubey D, Anamika K, Karmodiya K. 2018. Genome-wide survey and phylogenetic analysis of histone acetyltransferases and histone deacetylases of Plasmodium falciparum. FEBS J 285:1767–1782. https://doi.org/10.1111/febs.14376.
10. Hoeijmakers WAM, Miao J, Schmidt S, Toenhake CG, Shrestha S, Venhuizen J, Henderson R, Birnbaum J, Ghidelli-Disse S, Drewes G, Cui L, Stunnenberg HG, Spielmann T, Bártfai R. 2019. Epigenetic reader complexes of the human malaria parasite, Plasmodium falciparum. Nucleic Acids Res 47:11574–11588. https://doi.org/10.1093/nar/gkz1044.
11. Sen U, Saxena H, Khurana J, Nayak A, Gupta A. 2018. *Plasmodium falciparum* RUVBL3 protein: a novel DNA modifying enzyme and an interacting partner of essential HAT protein MYST. Sci Rep 8:10917. https://doi.org/10.1038/s41598-018-29137-8.
12. Barski A, Cuddapah S, Cui K, Roh T-Y, Schones DE, Wang Z, Wei G, Chepelev I, Zhao K. 2007. High-resolution profiling of histone methylations in the human genome. Cell 129:823–837. https://doi.org/10.1016/j.cell.2007.05.009.
13. Clarke AS, Lowell JE, Jacobson SJ, Pillus L. 1999. Esa1p is an essential histone acetyltransferase required for cell cycle progression. Mol Cell Biol 19:2515–2526. https://doi.org/10.1128/mcb.19.4.2515.
14. Bakshi K, Ranjitha B, Dubey S, Jagannadham J, Jaiswal B, Gupta A. 2017. Novel complex of HAT protein TIP60 and nuclear receptor PXR promotes cell migration and adhesion. Sci Rep 7:3635. https://doi.org/10.1038/s41598-017-03783-w.
15. Coffey K, Blackburn TJ, Cook S, Golding BT, Griffin RJ, Hardcastle IR, Hewitt L, Huberman K, McNeill HV, Newell DR, Roche C, Ryan-Munden CA, Watson A, Robson CN. 2012. Characterisation of a Tip60 specific inhibitor, NU9056, in prostate cancer. PLoS One 7:e45539. https://doi.org/10.1371/journal.pone.0045539.
16. Kirchner S, Power BJ, Waters AP. 2016. Recent advances in malaria genomics and epigenomics. Genome Med 8:92. https://doi.org/10.1186/s13073-016-0343-7.
17. Cortés A, Deitsch KW. 2017. Malaria epigenetics. Cold Spring Harb Perspect Med 7:a025528. https://doi.org/10.1101/cshperspect.a025528.
18. Duraisingh MT, Skillman KM. 2018. Epigenetic variation and regulation in malaria parasites. Annu Rev Microbiol 72:355–375. https://doi.org/10.1146/annurev-micro-090817-062722.
19. Gupta AP, Chin WH, Zhu L, Mok S, Luah YH, Lim EH, Bozdech Z. 2013.

Dynamic epigenetic regulation of gene expression during the life cycle of malaria parasite Plasmodium falciparum. PLoS Pathog 9:e1003170. https://doi.org/10.1371/journal.ppat.1003170.
20. Ay F, Bunnik EM, Varoquaux N, Vert JP, Noble WS, Le Roch KG. 2015. Multiple dimensions of epigenetic gene regulation in the malaria parasite Plasmodium falciparum: gene regulation via histone modifications, nucleosome positioning and nuclear architecture in P falciparum. Bioessays 37:182–194. https://doi.org/10.1002/bies.201400145.
21. Nguyen HHT, Yeoh LM, Chisholm SA, Duffy MF. 2020. Developments in drug design strategies for bromodomain protein inhibitors to target Plasmodium falciparum parasites. Expert Opin Drug Discov 15:415–-425. https://doi.org/10.1080/17460441.2020.1704251.
22. Chan A, Dziedziech A, Kirkman LA, Deitsch KW, Ankarklev J. 2020. A histone methyltransferase inhibitor can reverse epigenetically acquired drug resistance in the malaria parasite Plasmodium falciparum. Antimicrob Agents Chemother 64:e02021-19. https://doi.org/10.1128/AAC.02021-19.
23. Shimojo H, Sano N, Moriwaki Y, Okuda M, Horikoshi M, Nishimura Y. 2008. Novel structural and functional mode of a knot essential for RNA binding activity of the Esa1 presumed chromodomain. J Mol Biol 378:987–1001. https://doi.org/10.1016/j.jmb.2008.03.021.
24. Muralidharan V, Oksman A, Pal P, Lindquist S, Goldberg DE. 2012. *Plasmodium falciparum* heat shock protein 110 stabilizes the asparagine repeat-rich parasite proteome during malarial fevers. Nat Commun 3:1310. https://doi.org/10.1038/ncomms2306.
25. Filisetti D, Théobald-Dietrich A, Mahmoudi N, Rudinger-Thirion J, Candolfi E, Frugier M. 2013. Aminoacylation of Plasmodium falciparum tRNA(Asn) and insights in the synthesis of asparagine repeats. J Biol Chem 288:36361–36371. https://doi.org/10.1074/jbc.M113.522896.
26. Jha S, Gupta A, Dar A, Dutta A. 2013. RVBs are required for assembling a functional TIP60 complex. Mol Cell Biol 33:1164–-1174. https://doi.org/10.1128/MCB.01567-12.
27. Miao J, Lawrence M, Jeffers V, Zhao F, Parker D, Ge Y, Sullivan WJ, Jr, Cui L. 2013. Extensive lysine acetylation occurs in evolutionarily conserved metabolic pathways and parasite-specific functions during Plasmodium falciparum intraerythrocytic development. Mol Microbiol 89:660–675. https://doi.org/10.1111/mmi.12303.
28. Lehner B, Crombie C, Tischler J, Fortunato A, Fraser AG. 2006. Systematic mapping of genetic interactions in Caenorhabditis elegans identifies common modifiers of diverse signaling pathways. Nat Genet 38:896–903. https://doi.org/10.1038/ng1844.
29. Jaiswal B, Gupta A. 2018. Modulation of nuclear receptor function by chromatin modifying factor TIP60. Endocrinology 159:2199–2215. https://doi.org/10.1210/en.2017-03190.
30. Dekker FJ, van den Bosch T, Martin NI. 2014. Small molecule inhibitors of histone acetyltransferases and deacetylases are potential drugs for inflammatory diseases. Drug Discov Today 19:654–660. https://doi.org/10.1016/j.drudis.2013.11.012.
31. Yang C, Ngo L, Zheng YG. 2014. Rational design of substrate-based multivalent inhibitors of the histone acetyltransferase Tip60. ChemMedChem 9:537–541. https://doi.org/10.1002/cmdc.201300478.
32. Cheng Y, He C, Wang M, Ma X, Mo F, Yang S, Han J, Wei X. 2019. Targeting epigenetic regulators for cancer therapy: mechanisms and advances in clinical trials. Signal Transduct Target Ther 4:62. https://doi.org/10.1038/s41392-019-0095-0.
33. Ganesan A, Arimondo PB, Rots MG, Jeronimo C, Berdasco M. 2019. The timeline of epigenetic drug discovery: from reality to dreams. Clin Epigenetics 11:174. https://doi.org/10.1186/s13148-019-0776-0.
34. Song Y, DiMaio F, Wang RY-R, Kim D, Miles C, Brunette T, Thompson J, Baker D. 2013. High-resolution comparative modeling with RosettaCM. Structure 21:1735–1742. https://doi.org/10.1016/j.str.2013.08.005.
35. Sali A, Blundell TL. 1993. Comparative protein modelling by satisfaction of spatial restraints. J Mol Biol 234:779–-815. https://doi.org/10.1006/jmbi.1993.1626.
36. Waterhouse A, Bertoni M, Bienert S, Studer G, Tauriello G, Gumienny R, Heer FT, de Beer TAP, Rempfer C, Bordoli L, Lepore R, Schwede T. 2018. SWISS-MODEL: homology modelling of protein structures and complexes. Nucleic Acids Res 46:W296–W303. https://doi.org/10.1093/nar/gky427.
37. Pettersen EF, Goddard TD, Huang CC, Couch GS, Greenblatt DM, Meng EC, Ferrin TE. 2004. UCSF Chimera–a visualization system for exploratory research and analysis. J Comput Chem 25:1605–-1612. https://doi.org/10.1002/jcc.20084.